JACS
JOURNAL OF THE AMERICAN CHEMICAL SOCIETY
Article
pubs.acs.org/JACS

Molecular Location Sensing Approach by Anisotropic Magnetism of an Endohedral Metallofullerene

Yuta Takano,[*,†] Ryo Tashita,[‡] Mitsuaki Suzuki,[‡,§] Shigeru Nagase,[*,∥] Hiroshi Imahori,[†,⊥] and Takeshi Akasaka[*,‡,§,#,∇]

[†]Institute for Integrated Cell-Material Sciences (WPI-iCeMS), Kyoto University, Sakyo-ku, Kyoto 606-8501, Japan
[‡]Life Science Center of Tsukuba Advanced Research Alliance, University of Tsukuba, Tsukuba, Ibaraki 305-8577, Japan
[§]Department of Chemistry, Tokyo Gakugei University, Tokyo 184-8501, Japan
[∥]Fukui Institute for Fundamental Chemistry, Kyoto University, Sakyo-ku, Kyoto 606-8103, Japan
[⊥]Department of Molecular Engineering, Graduate School of Engineering, Kyoto University, Nishikyo-ku, Kyoto 615-8510, Japan
[#]State Key Laboratory of Materials Processing and Die & Mold Technology, School of Materials Science and Technology, Huazhong University of Science and Technology, Wuhan 430074, China
[∇]Foundation for Advancement of International Science, Tsukuba, Ibaraki 305-0821, Japan

Supporting Information

ABSTRACT: Location recognition at the molecular scale provides valuable information about the nature of functional molecular materials. This study presents a novel location sensing approach based on an endohedral metallofullerene, Ce@C_{82}, using its anisotropic magnetic properties, which lead to temperature-dependent paramagnetic shifts in ^{1}H NMR spectra. Five site-isomers of Ce@$C_{82}CH_2$-3,5-$C_6H_3Me_2$ were synthesized to demonstrate the spatial sensing ability of Ce@C_{82}. Single-crystal structures, absorption spectra, and density functional theory calculations were used to select the plausible addition positions in the radical coupling reaction, which preferentially happens on the carbon atoms with high electron density of the singly occupied molecular orbital (SOMO) and positive charge. Temperature-dependent NMR measurements demonstrated unique paramagnetic shifts of the ^{1}H peaks, which were derived from the anisotropic magnetism of the f-electron in the Ce atom of the isomers. It was found that the magnetic anisotropy axes can be easily predicted by theoretical calculations using the Gaussian 09 package. Further analysis revealed that the temperature-dependent trend in the shifts is clearly predictable from the distance and relative position of the proton from the Ce atom. Hence, the Ce-encapsulated metallofullerene Ce@C_{82} can provide spatial location information about nearby atoms through the temperature-dependent paramagnetic shifts of its NMR signals. It can act as a molecular probe for location sensing by utilizing the anisotropic magnetism of the encapsulated Ce atom. The potentially low toxicity and stability of the endohedral fullerene would make Ce@C_{82} suitable for applications in biology and material science.

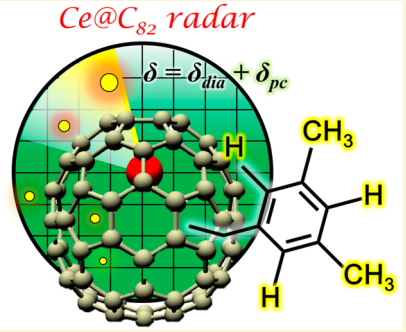

INTRODUCTION

Spatial location recognition at the molecular scale provides valuable information on the spatial relationship, absolute conformation, and dynamics of molecules. This information is essential for elucidating biological processes[1−3] and understanding the nature of functional molecular materials.[4−6] A number of methods have been developed and reported for molecular recognition and location determination. For example, the location information on atoms in nanomaterials and proteins can be obtained by standard spectroscopic methods,[4,5] crystallographic methods,[1−3,6] cryo-electron microscopy,[7,8] photo labeling,[9] and the analysis of nuclear magnetic resonance (NMR) chemical shifts.[10−12] However, their effectiveness is limited by the required relatively high affinity for the probe, or the weak acquired signals.

Ligand-transferred paramagnetic NMR restraints for location identification have been studied as an attractive method for investigating drugs and drug candidates with potentially low affinity.[12,13] The shift reagents for this purpose generally consist of complex ligands and lanthanoid or actinoid atoms, to utilize the unique characteristic of electrons in the f orbitals of these metal atoms. These ligands, however, are not expected to be suitable for harsh conditions, because they can decompose with time and/or at high temperature. Neither are they suitable for living organisms as the reagents may be cytotoxic.[14]

Recently, our group reported anisotropic magnetism in an endohedral metallofullerene (EMF) Ce@C_{2v}-C_{82} (hereafter denoted as Ce@C_{82}, "C_{2v}" and "@" indicate the molecular

Received: April 26, 2016
Published: June 17, 2016

DOI: 10.1021/jacs.6b04037
J. Am. Chem. Soc. 2016, 138, 8000−8006

symmetry of the fullerene cage and encapsulation, respectively) in both the pristine form[15,16] and the chemically functionalized form.[17] Remarkably, the observed magnetic anisotropy in NMR measurements was weakly influenced by the addition of a carbene. Moreover, the absolute positions of the hydrogen atoms of the addend could be assigned by analyzing the effective distance in the anisotropic magnetism, which decreases with the cube of the distance between the Ce and hydrogen atoms. Thus, it was evident that Ce@C_{82} can act as a distance detector for the surrounding atoms and addends.

EMFs are promising candidates for spatial location detection, because the caged metal is isolated from the outer environment and rarely escapes from the fullerene cage even in extreme conditions, such as high temperature and strongly acidic or basic media.[18−20] Such stability makes them the preferred molecular probes in a variety of materials ranging from biological systems to industrial chemicals, which require low toxicity and high durability. Nevertheless, the practical application of EMFs has been limited because their synthetic yields are generally quite low. To overcome this problem, several research groups have developed efficient methods to produce and purify EMFs in higher amounts.[21,22]

Another challenge for utilizing EMFs as molecular location probes is the lack of understanding of the effects of the anisotropic magnetism on positions other than on the top part of the fullerene cage. It is also desirable to clarify the influence of addends other than carbene on the anisotropic magnetism, to create high-performance EMF-based probes by chemical modification. In addition, the influence from the dynamic motion of the vicinal atoms, which can be observed in singly bonded derivatives for instance, should be elucidated to provide a basis for detecting the dynamic atoms in biological molecules such as proteins, DNAs, and RNAs.

In this study, we have developed Ce@C_{82} derivatives and demonstrated the necessary properties as a new type of molecular probes for location recognition. They are capable of detecting not only the relative distance, but also the relative position with regard to the Ce atom probe, by correlating the experimentally observed anisotropic magnetism of the EMF with the molecular structures and electronic properties from theoretical computations.

RESULTS AND DISCUSSION

Molecular Design and Synthesis. Radical adducts of Ce@C_{82} were chosen as the target molecules for elucidating the anisotropic magnetic property toward location recognition (Scheme 1). It is because (i) Ce@C_{82} can be a simple spin model with a single f-electron for elucidating the anisotropic magnetic properties, (ii) a radical reaction method has been established for La@C_{82},[23,24] which has chemical reactivity similar to that of Ce@C_{82}, and a limited number of monosubstituted site-isomers are expected to be afforded; (iii) the addition sites for two site-isomers have already been identified for La@C_{82}; (iv) some of the addition sites are on the side instead of the top of the fullerene cage; and (v) the resulting adducts can be readily observed in NMR because of the diamagnetic property of the fullerene cage due to the radical addition. The pristine cage of Ce@C_{82} or La@C_{82} is paramagnetic as a result of electron transfer from the metal to the cage.[18−20] Therefore, these fullerenes must be electrochemically reduced by one electron to acquire NMR signals.[15,25] Radical coupling reaction has the advantage of directly affording diamagnetic compounds,[23] without further electrochemical reduction, which is required in conventional cycloaddition reactions of fullerenes, such as the Prato reactions[18,26] or the Diels−Alder reactions.[20]

Scheme 1. Synthetic Scheme of M@C_{82} (M = Ce or La)

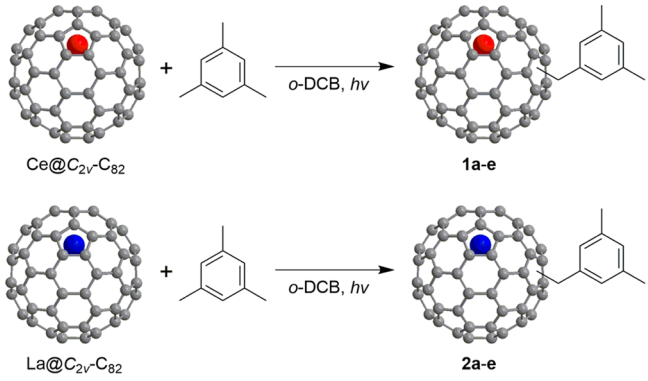

The target compounds were synthesized by photoirradiation ($h\nu$ > 330 nm) of Ce@C_{82} in the presence of mesitylene (Figure 1a). Photoinduced cleavage of alpha hydrogen of mesitylene

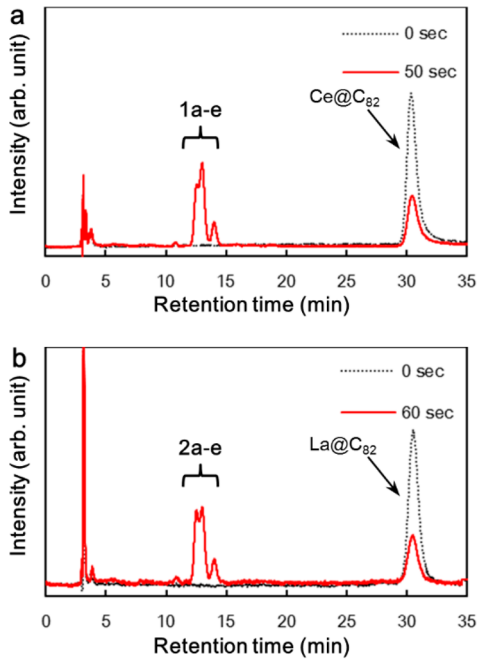

Figure 1. (a) HPLC profiles of the mixtures of **1a−e**, before (black line) and after (red line) 50 s of photoreaction. (b) HPLC profiles of the photoreaction mixtures for **2a−e**.

triggers the radical coupling between the resulting radical $C_6H_3Me_2CH_2^{\bullet}$ and Ce@C_{82}. Multistep high-performance liquid chromatography (HPLC) separation afforded five isomers (**1a−e**) (see also Figures S1 and S2), four of which (**1b−e**) correspond to the four isomers previously reported in monobenzyl adducts of La@C_{82},[23] and one additional isomer (**1a**). The corresponding lanthanum compounds **2a−e** were also synthesized by using La@C_{82} instead of Ce@C_{82} as diamagnetic reference molecules for comparison (Figures 1b, S3, and S4).

Vis−near IR absorption spectra provided information on the molecular structures of **1a−e** and **2a−e** (Figures S5 and S6). It is generally known that similar absorption spectra of fullerene derivatives in the vis−near IR region indicate the same position of the addend on the fullerene cage. This allows us to conclude

DOI: 10.1021/jacs.6b04037
J. Am. Chem. Soc. 2016, 138, 8000−8006

that the compounds **1a−e** and **2a−e** have one-to-one correspondence. The molecular structure of **1d** was successfully elucidated by single-crystal X-ray diffraction analysis (SCXRD), in which the 3,5-dimethyl-benzyl group is attached to C10 (Figure 2a and b). This is the same position as that of a reported

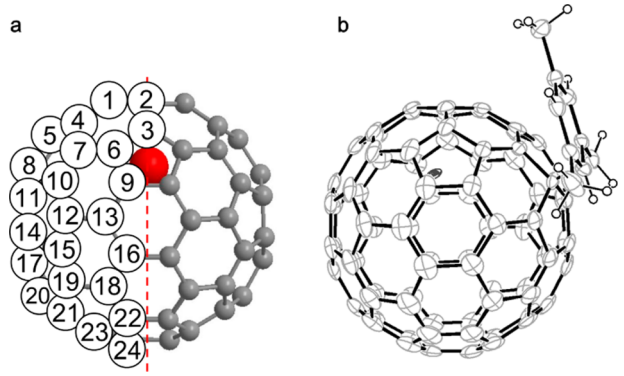

Figure 2. (a) Schematic drawing of M@C_{82} with the carbon atoms numbered. Red dashed line indicates the C_{2v} axis. (b) Molecular structure of **1d** drawn by the ORTEP program with 30% thermal ellipsoids. The solvent and minor metal positions are omitted for clarity.

benzyl adduct of La@C_{82} identified by single-crystal structure.[23] The addition positions of **1e** and **2e** were determined to be both C23, based on the resemblance of their absorption spectra to that reported for the singly bonded La@C_{82} derivative.[27] These results will provide essential information for deducing the location of the addends by NMR measurements utilizing anisotropic magnetism (vide infra).

Density Functional Theory Calculations of Plausible Addition Positions. Density functional theory (DFT) provides a reasonable way to determine the addition positions in the radical coupling reaction.[23] The spin densities derived from the singly occupied molecular orbital (SOMO) of the carbon atoms in Ce@C_{82} were calculated using the Gaussian 09 program.[28] Eight carbon atoms with the highest spin densities (C2, C3, C9, C10, C14, C18, C19, and C23; Table 1) were selected as candidate positions for the radical addition, which is expected to occur on the atoms with the highest spin density. It is generally known that the aryl radicals without electron-withdrawing groups are relatively nucleophilic, and prefer to undergo radical coupling with an electron-deficient atom. This is also true in the case of fullerenes.[23,29] Among them, positions C2 and C3 can be excluded, because the addition at either position leads to C_s molecular symmetry, while the NMR spectra indicate C_1 symmetry. Their negative Mulliken charges (C2 −0.209, C3 −0.132) further support their exclusion from consideration. C19 can be also excluded, based on the fact that the carbon atom is negatively charged, and addition to this position would result in the most unstable adduct (+4.5 kcal/mol higher than the most stable adduct). Among the remaining five plausible positions (C9, C10, C14, C18, and C23, Figure S7), C10 and C23 were experimentally verified as the addition positions of **1d** and **1e** respectively, as discussed above. This consistency supports the validity of DFT predictions.

Table 1. Eight Carbon Atom Positions in the Pristine Ce@C_{2v}-C_{82} with the Highest SOMO Spin Densities, Their Mulliken Charges, and the Relative Energies of Formation of Ce@$C_{82}CH_2$-3,5-$C_6H_3Me_2$ from DFT Calculations[a]

carbon number	resulting symmetry	spin density	Mulliken charge[b]	relative energy (kcal/mol)
C10	C_1	0.031	+0.003	0.3
C18	C_1	0.030	+0.005	0.4
C23	C_1	0.025	+0.008	0.0
C19	C_1	0.025	−0.004	4.5
C3	C_s	0.025	−0.132	0.9
C9	C_1	0.024	+0.005	2.7
C2	C_s	0.023	−0.209	2.6
C14	C_1	0.021	+0.004	0.1

[a]Calculated at the B3LYP/6-31G* [C and H], SDD [Ce]//B3LYP/3-21G [C and H], SDD [Ce] level. [b]Calculated at the B3LYP/3-21G [C and H], SDD [Ce] level.

Temperature-Dependent ^{1}H NMR Spectra. The paramagnetic shifts in ^{1}H NMR signals were recorded at various temperatures. The chemical shifts of **1a−d** exhibited temperature-dependent (TD) changes that originate from the f-electron spin remaining on Ce^{3+} ($4f^15d^06s^0$) in the cage (Figures 4a, S8−11). The signals of **1e** were not detectable because of the low yield of this compound. The chemical shift (δ) of a paramagnetic molecule in solution is generally expressed as the sum of three contributions, the diamagnetic (δ_{dia}), Fermi contact (δ_{fc}), and pseudocontact (δ_{pc}) shifts:

$$\delta = \delta_{dia} + \delta_{fc} + \delta_{pc} \quad (1)$$

The δ_{dia} values of **1a−d** were obtained from the corresponding chemical shifts of **2a−d**. In recent literature, it was demonstrated that δ_{pc} dominates the TD shift for various nuclear species such as ^{1}H, ^{13}C, and ^{45}Sc in the EMFs with f-electron spin, and δ_{fc} contributes little to the shift.[15−17,30,31] The δ_{pc} term can be briefly described as

$$\delta_{pc} = \frac{C(3\cos^2\theta - 1)}{r^3T^2} \quad (2)$$

where T is the measurement temperature, r is the magnitude of the **r** vector as well as the distance between the Ce atom and the atom of interest (Figure 3a), and θ is the angle between the **r** vector and the axis defined by the molecule (which will be discussed in the next subsection). C is a common constant, which can be estimated experimentally (-2.1×10^7 Å^3 K^2 in the present case). r can be fixed by the experimentally or theoretically determined molecular structures, with the positions of the atoms averaged to take into account the dynamic rotation of the addend. Therefore, one can expect that the amplitude of δ_{pc}

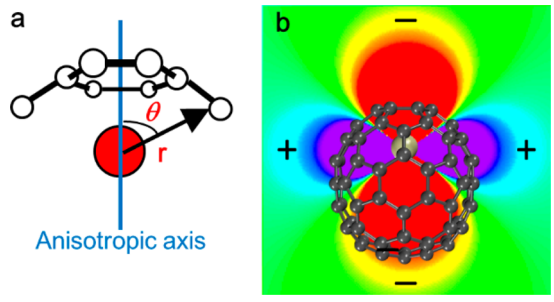

Figure 3. (a) Definition of the distance (r) based on the **r** vector, anisotropic axis, and angle (θ) in eq 2. (b) Two-dimensional plots of the effective field of anisotropic magnetism derived from the δ_{pc} value of the Ce atom. The red, green, and blue areas display high-field, neutral, and low-field shift effects in NMR measurements, respectively.

DOI: 10.1021/jacs.6b04037
J. Am. Chem. Soc. 2016, 138, 8000−8006

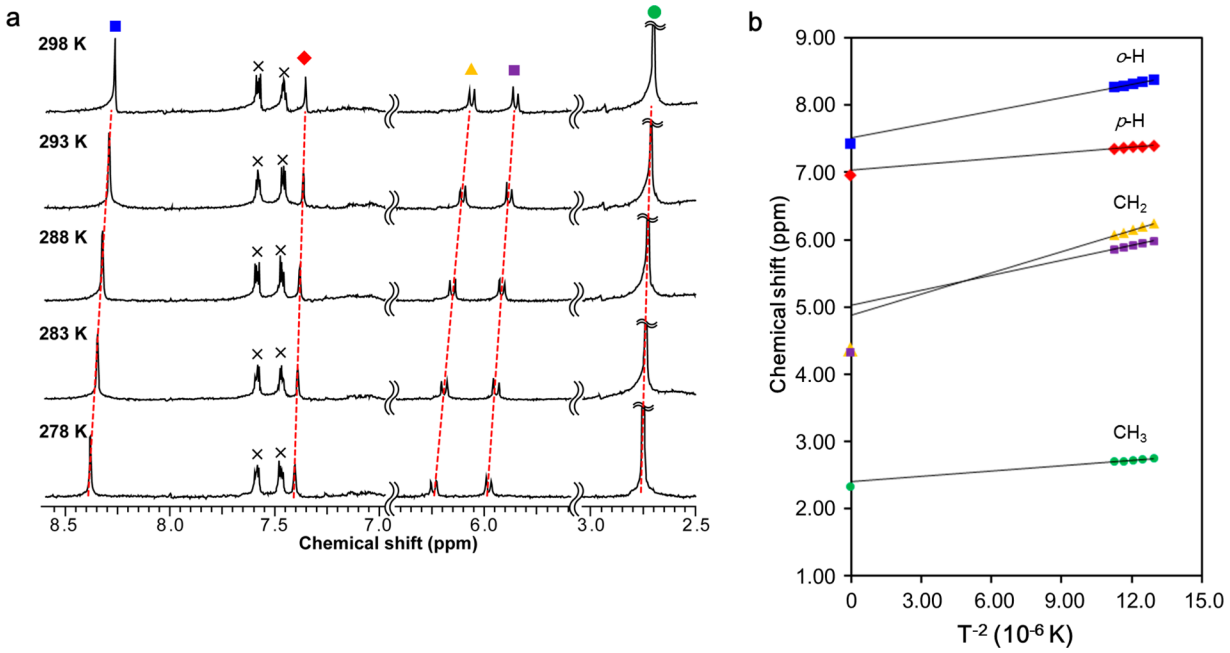

Figure 4. (a) TD ^{1}H NMR spectra at various temperatures. The ×-marks indicate the temperature-independent signals of dibutyl phthalate for highlighting the other TD signals. (b) Plots of the ^{1}H NMR measurements with linear fitting, demonstrating the dependence of the chemical shifts on T^{-2}. The plotted values at $T^{-2} = 0$ are the observed chemical shifts in **2d** recorded at room temperature, which are theoretically expected to be the same as the shifts of **1d** at $T^{-2} = 0$.

varies with the distance and the relative position from the Ce atom (Figure 3b), which is the key to molecular location sensing.

In the case of **1d**, four signals including one AB quartet were observed, indicating C_1 symmetry (Figure 4a). Remarkably, the shifts of the signals changed with temperature. The plot of the chemical shifts versus T^{-2} (Figure 4b) demonstrates the temperature dependence of the anisotropic magnetism derived from the Ce atom. The consistency between the extrapolated *y*-intercepts and the observed chemical shifts of **2d** recorded at room temperature (plotted at $T^{-2} = 0$ in Figure 4b), which are theoretically expected to be the same as the shifts of **1d** at $T^{-2} = 0$, confirms that the shifts are dominated by δ_{pc}, regardless of the dynamic motion of the protons. Exceptions are the two methylene proton signals (orange and purple), extrapolated intercepts of which deviate considerably from corresponding signals of diamagnetic reference **2d**. Because the two protons are distant enough from the Ce atom (5.8 Å) as in the case of previous reported Ce encapsulated fullerenes and their derivatives,[17] this may not be attributed to the contribution of δ_{fc} as supported by the large deviation shown in the dependency for T^{-1} (Figure S13), but to an uncertain dynamic effect to be investigated.

Utilizing Anisotropic Magnetism for Location Sensing. The paramagnetic shifts in the NMR spectra were further investigated to clarify the influence of the anisotropic magnetism on location sensing. In the case of **1d**, the addition position has been experimentally determined as C10. The observed temperature dependence of chemical shifts on T^{-2}, $C(3\cos^2\theta - 1)/r^3$ obtained from linear fitting (Figure 4b), was compared to the calculated values based on eq 2 with the single-crystal structure and three different axis systems (Figure 5a and b). Specifically, the three axes are (i) the original C_{2v} axis in the pristine Ce@C_{82} (Figure 5a and b, blue, labeled as "original"), (ii) the axis along the local electric field predicted by DFT calculations (Figure 5a and b, red, labeled as "EF"), and (iii) the axis connecting the Ce atom and the carbon atom of the addition position (Figure 5a and b, orange, labeled as "addend"). Here, we found that the EF axis system can reasonably reproduce the anisotropic magnetic axes of not only pristine Ce@C_{82} and a previously reported Ce@

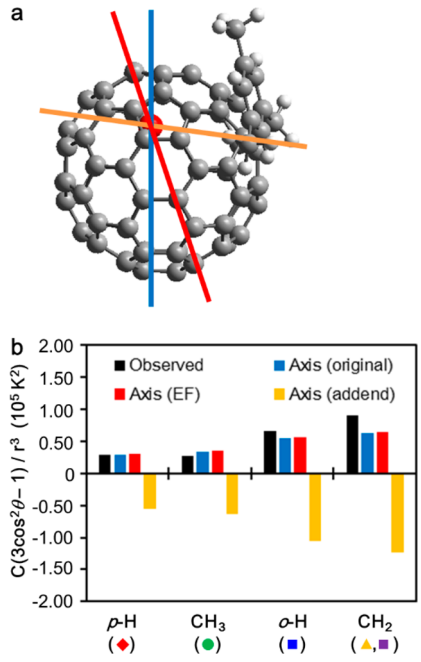

Figure 5. (a) The SCXRD structure of **1d**, showing the three possible definitions of the axis. Blue line: the axis parallel to the original C_{2v} axis of the pristine Ce@C_{82}. Red line: the axis along the direction of the local electric field predicted by the DFT calculation. Orange line: the axis connecting the Ce atom and the addition position. (b) The temperature dependence of ^{1}H NMR signals to T^{-2} obtained from Figure 4b. The black bars indicate the observed values, and the values calculated using each of the axes in (a) are colored accordingly.

DOI: 10.1021/jacs.6b04037
J. Am. Chem. Soc. 2016, 138, 8000−8006

Table 2. Statistical Analysis of the Observed Paramagnetic Shifts in the ^{1}H NMR Signals of Compound 1d in Figure 5b for Different Addend Locations

compound	addition position	structure	axis system	Pearson product−moment correlation coefficient (r_p)	p-value for t-test	R^2
1d	C10	SCXRD	original	0.98	0.84	0.96
			EF	0.98	1.00	0.96
			addend	−0.98	0.06	0.97
	C9	DFT	original	0.98	0.31	0.96
			EF	0.97	0.14	0.93
			addend	−0.98	0.05	0.96
	C10	DFT	original	0.98	0.87	0.97
			EF	0.98	0.91	0.97
			addend	−0.98	0.06	0.97
	C14	DFT	original	0.98	0.15	0.96
			EF	−0.99	0.10	0.98
			addend	−0.98	0.05	0.96
	C18	DFT	original	−0.99	0.09	0.97
			EF	−0.99	0.09	0.97
			addend	−0.27	0.01	0.97

C_{82} derivative (Figures S14 and S15),[15,17] but also $[Dy(paaH^*)_2(H_2O)_4]_3$ (Figure S16).[32,33] The trends in the NMR signals of **1d** and the calculated values based on its crystal structure and the DFT optimized structures were statistically analyzed by the Pearson product−moment correlation coefficient (r_p), p values for the paired t-test, and R^2 values from linear fitting, and the results are listed in Table 2. The definition for r_p is described in eq 3, and positive values close to +1.00 indicate high relevance between the two groups of values (x and y) of interest.

$$r_p = \frac{\sum (x - \bar{x})(y - \bar{y})}{\sqrt{\sum (x - \bar{x})^2 \sum (y - \bar{y})^2}} \quad (3)$$

It was found that the correlation coefficients can serve as an initial filter to eliminate impossible addition positions and axis system, which have negative correlation coefficients. The most probable addition position then can be selected by the highest p value. It is C10 in the case using the DFT optimized structures, being in agreement with the experimental result. Meanwhile, the R^2 values do not seem to be highly relevant in determining the addition position. The EF axis was confirmed to best reproduce the experimental result, although the original C_{2v} axis could also reproduce it in the case of **1d**, due to the similar directions of the two axes. The third axis ("addend") was found unsuitable for this purpose. Hence, we conclude that the addend position can be determined by a detailed examination of the experimental TD shifts, using theoretically predicted molecular structures, the EF axis system, and statistical analysis. In addition, calculating from eq 2, the effective range is 13.3 Å for $\delta_{pc} = -0.2$ ppm at 298 K to occur for the proton on the anisotropic axis. It is sufficient range to cover the mesityl addend of compounds **1a**−**c**.

For **1a**−**c**, the trends of their TD shifts in ^{1}H NMR are quite different (Figures S8−S10). **1a** shows only high-field shifts with increasing temperature, whereas **1b** and **1c** show mixed shifts, reflecting the distinct addition positions from those of **1a** and **1d**. The addition positions in **1a**−**c** were determined by the same statistical analysis method as for **1d** (Figure S17, Tables 3 and S2). The correlation coefficients and p values were systematically examined for all three candidate addition positions discussed above (C9, C14, and C18). As a result, the addition positions were successfully determined as C9 for **1a**, C14 for **1b**, and C18 for **1c**. These results evidence that the paramagnetic shifts based on the anisotropic magnetism of the encapsulated Ce atom can be used for molecular location sensing.

Table 3. Determination of the Addend Locations in 1a−d by Statistical Analysis, Using DFT-Optimized Structures and the EF Axis

compound	r_p	p-value for t-test	addition position
1a	0.98	0.07	C9
1b	0.99	0.84	C14
1c	0.15	0.32	C18
1d	0.98	0.91	C10

CONCLUSION

Five radical adducts of Ce@C_{82} (**1a**−**e**) were successfully designed and synthesized to demonstrate the feasibility of using Ce@C_{82} as a probe for molecular location recognition, using the TD chemical shifts in their ^{1}H NMR signals from the anisotropic magnetism of the Ce atom. A detailed numerical analysis of the shifts using statistical criteria enabled us to determine the locations of nearby atoms relative to the fullerene cage in all of the adducts. One can anticipate that chemical modification in or on the fullerene cage will achieve further improvement of the EMF-based molecular probe. These molecular location probes would be applied in many areas, such as biology, nanoscience, and material science under a variety of conditions.

EXPERIMENTAL PROCEDURES

General. All chemicals and solvents were obtained from Wako Inc. or Sigma-Aldrich Inc. and used without further purification unless otherwise stated. La@C_{2v}-C_{82}[34] and Ce@C_{2v}-C_{82}[35] were prepared according to the reported procedures. 1,3,5-Trimethylbenzene (mesitylene) and o-DCB were distilled over benzophenone sodium ketyl under an argon atmosphere prior to use in a reaction. Analytical high-performance liquid chromatography (HPLC) was performed on a series of HPLC apparatus (Jasco Inc.) using 5PYE, Buckyprep, or 5PBB columns (4.6 × 250 mm; Nacalai Tesque Inc.). Preparative HPLC was performed on a HPLC apparatus LC-908 C_{60} (Japan Analytical Industry Inc.) using 5PYE, Buckyprep, or 5PBB columns (20 × 250 mm; Nacalai Tesque Inc.). Monitoring absorption was carried out at 330 nm, and toluene was used as an eluent for HPLC. The ^{1}H NMR measurements were conducted on a spectrometer (AVANCE 500; Bruker Analytik GmbH) with a CryoProbe system, where TMS was used as an internal reference (δ = 0.00 ppm). Absorption spectra were recorded using a spectrophotometer (UV-3150; Shimadzu Corp.). Mass spectrometry

DOI: 10.1021/jacs.6b04037
J. Am. Chem. Soc. 2016, 138, 8000−8006

was conducted using a mass spectrometer (BIFLEX III; Bruker Analytik GmbH) with 1,1,4,4-tetraphenyl-1,3-butadiene as a matrix.

Theoretical Calculations. All theoretical calculations were conducted using the Gaussion 09 revision D.01 program.[28] A computing method and level of theory for the present study was selected as unrestricted B3LYP[36] as a functional and 3-21G[37] for structural optimizations and 6-31G(d)[38] for single point calculations as a basis set with the SDD relativistic effective core potential[39] for the metal atoms, after the advance verifications (see the Supporting Information for details). Anisotropic axis derived from a metal atom was predicted by the local electric field around the atom, which was calculated by the Gaussian 09 package as electrostatic properties using the "Prop" keyword.[40]

Statistic Analyses. The Pearson product−moment correlation coefficients (r_p), double-tailed p values for the paired t-test, and R^2 values from linear fitting were calculated by using Microsoft Excel 2013 software.

■ ASSOCIATED CONTENT

Supporting Information

The Supporting Information is available free of charge on the ACS Publications website at DOI: 10.1021/jacs.6b04037.

Detailed synthetic procedures, spectroscopic data for all new compounds, supplementary characterizations and analyses, and optimized structures from theoretical calculations(PDF)

X-ray data for compound **2d** (CIF)

■ AUTHOR INFORMATION

Corresponding Authors

*ytakano@icems.kyoto-u.ac.jp

*nagase@ims.ac.jp

*akasaka@tara.tsukuba.ac.jp

Notes

The authors declare no competing financial interest.

■ ACKNOWLEDGMENTS

We thank Prof. M. M. Olmstead and Prof. A. L. Balch for their helpful advice to analyze the crystal structure. This work is supported by financial supports from research on Innovative Areas (20108001, "π-Space") and Grants-in-Aid for Scientific Research (C) (15K05563), MEXT, Japan. The iCeMS is supported by World Premier International Research Center Initiative (WPI), MEXT, Japan.

■ REFERENCES

(1) Rohs, R.; West, S. M.; Sosinsky, A.; Liu, P.; Mann, R. S.; Honig, B. *Nature* **2009**, *461*, 1248−1253.

(2) Jiang, C. Z.; Pugh, B. F. *Nat. Rev. Genet.* **2009**, *10*, 161−172.

(3) Davey, C. A.; Sargent, D. F.; Luger, K.; Maeder, A. W.; Richmond, T. J. *J. Mol. Biol.* **2002**, *319*, 1097−1113.

(4) Beaujuge, P. M.; Frechet, J. M. J. *J. Am. Chem. Soc.* **2011**, *133*, 20009−20029.

(5) Ratera, I.; Veciana, J. *Chem. Soc. Rev.* **2012**, *41*, 303−349.

(6) Guillerm, V.; Kim, D.; Eubank, J. F.; Luebke, R.; Liu, X.; Adil, K.; Lah, M. S.; Eddaoudl, M. *Chem. Soc. Rev.* **2014**, *43*, 6141−6172.

(7) Bartesaghi, A.; Merk, A.; Banerjee, S.; Matthies, D.; Wu, X. W.; Milne, J. L. S.; Subramaniam, S. *Science* **2015**, *348*, 1147−1151.

(8) da Fonseca, P. C. A.; Morris, E. P. *Nat. Commun.* **2015**, *6*, 7573.

(9) Tamura, T.; Kioi, Y.; Miki, T.; Tsukiji, S.; Hamachi, I. *J. Am. Chem. Soc.* **2013**, *135*, 6782−6785.

(10) Bottrill, M.; Nicholas, L. K.; Long, N. J. *Chem. Soc. Rev.* **2006**, *35*, 557−571.

(11) Otting, G. *Annu. Rev. Biophys.* **2010**, *39*, 387−405.

(12) Brath, U.; Swamy, S. I.; Veiga, A. X.; Tung, C. C.; Van Petegem, F.; Erdelyi, M. *J. Am. Chem. Soc.* **2015**, *137*, 11391−11398.

(13) Clore, G. M.; Iwahara, J. *Chem. Rev.* **2009**, *109*, 4108−4139.

(14) Hirano, S.; Suzuki, K. T. *Environ. Health Perspect.* **1996**, *104*, 85−95.

(15) Yamada, M.; Wakahara, T.; Lian, Y. F.; Tsuchiya, T.; Akasaka, T.; Waelchli, M.; Mizorogi, N.; Nagase, S.; Kadish, K. M. *J. Am. Chem. Soc.* **2006**, *128*, 1400−1401.

(16) Yamada, M.; Mizorogi, N.; Tsuchiya, T.; Akasaka, T.; Nagase, S. *Chem. - Eur. J.* **2009**, *15*, 9486−9493.

(17) Takano, Y.; Aoyagi, M.; Yamada, M.; Nikawa, H.; Slanina, Z.; Mizorogi, N.; Ishitsuka, M. O.; Tsuchiya, T.; Maeda, Y.; Akasaka, T.; Kato, T.; Nagase, S. *J. Am. Chem. Soc.* **2009**, *131*, 9340−9346.

(18) Popov, A. A.; Yang, S. F.; Dunsch, L. *Chem. Rev.* **2013**, *113*, 5989−6113.

(19) Nagase, S. *Bull. Chem. Soc. Jpn.* **2014**, *87*, 167−195.

(20) Yamada, M.; Akasaka, T. *Bull. Chem. Soc. Jpn.* **2014**, *87*, 1289−1314.

(21) Stevenson, S.; Harich, K.; Yu, H.; Stephen, R. R.; Heaps, D.; Coumbe, C.; Phillips, J. P. *J. Am. Chem. Soc.* **2006**, *128*, 8829−8835.

(22) Akiyama, K.; Hamano, T.; Nakanishi, Y.; Takeuchi, E.; Noda, S.; Wang, Z. Y.; Kubuki, S.; Shinohara, H. *J. Am. Chem. Soc.* **2012**, *134*, 9762−9767.

(23) Takano, Y.; Yomogida, A.; Nikawa, H.; Yamada, M.; Wakahara, T.; Tsuchiya, T.; Ishitsuka, M. O.; Maeda, Y.; Akasaka, T.; Kato, T.; Slanina, Z.; Mizorogi, N.; Nagase, S. *J. Am. Chem. Soc.* **2008**, *130*, 16224−16230.

(24) Takano, Y.; Ishitsuka, M. O.; Tsuchiya, T.; Akasaka, T.; Kato, T.; Nagase, S. *Chem. Commun.* **2010**, *46*, 8035−8036.

(25) Akasaka, T.; Wakahara, T.; Nagase, S.; Kobayashi, K.; Waelchli, M.; Yamamoto, K.; Kondo, M.; Shirakura, S.; Okubo, S.; Maeda, Y.; Kato, T.; Kako, M.; Nakadaira, Y.; Nagahata, R.; Gao, X.; Van Caemelbecke, E.; Kadish, K. M. *J. Am. Chem. Soc.* **2000**, *122*, 9316−9317.

(26) Maggini, M.; Scorrano, G.; Prato, M. *J. Am. Chem. Soc.* **1993**, *115*, 9798−9799.

(27) Feng, L.; Nakahodo, T.; Wakahara, T.; Tsuchiya, T.; Maeda, Y.; Akasaka, T.; Kato, T.; Horn, E.; Yoza, K.; Mizorogi, N.; Nagase, S. *J. Am. Chem. Soc.* **2005**, *127*, 17136−17137.

(28) Frisch, M. J.; Trucks, G. W.; Schlegel, H. B.; Scuseria, G. E.; Robb, M. A.; Cheeseman, J. R.; Scalmani, G.; Barone, V.; Mennucci, B.; Petersson, G. A.; Nakatsuji, H.; Caricato, M.; Li, X.; Hratchian, H. P.; Izmaylov, A. F.; Bloino, J.; Zheng, G.; Sonnenberg, J. L.; Hada, M.; Ehara, M.; Toyota, K.; Fukuda, R.; Hasegawa, J.; Ishida, M.; Nakajima, T.; Honda, Y.; Kitao, O.; Nakai, H.; Vreven, T.; Montgomery, J. A., Jr.; Peralta, J. E.; Ogliaro, F.; Bearpark, M.; Heyd, J. J.; Brothers, E.; Kudin, K. N.; Staroverov, V. N.; Kobayashi, R.; Normand, J.; Raghavachari, K.; Rendell, A.; Burant, J. C.; Iyengar, S. S.; Tomasi, J.; Cossi, M.; Rega, N.; Millam, J. M.; Klene, M.; Knox, J. E.; Cross, J. B.; Bakken, V.; Adamo, C.; Jaramillo, J.; Gomperts, R.; Stratmann, R. E.; Yazyev, O.; Austin, A. J.; Cammi, R.; Pomelli, C. J.; Ochterski, W.; Martin, R. L.; Morokuma, K.; Zakrzewski, V. G.; Voth, G. A.; Salvador, P.; Dannenberg, J. J.; Dapprich, S.; Daniels, A. D.; Farkas, O.; Foresman, J. B.; Ortiz, J. V.; Cioslowski, J. *Gaussian 09*, revision D.01; Gaussian, Inc.: Wallingford, CT, 2009.

(29) Morton, J. R.; Negri, F.; Preston, K. F. *Acc. Chem. Res.* **1998**, *31*, 63−69.

(30) Wang, X. L.; Zuo, T. M.; Olmstead, M. M.; Duchamp, J. C.; Glass, T. E.; Cromer, F.; Balch, A. L.; Dorn, H. C. *J. Am. Chem. Soc.* **2006**, *128*, 8884−8889.

(31) Zhang, Y.; Krylov, D.; Rosenkranz, M.; Schiemenz, S.; Popov, A. A. *Chem. Sci.* **2015**, *6*, 2328−2341.

(32) Chilton, N. F.; Collison, D.; McInnes, E. J. L.; Winpenny, R. E. P.; Soncini, A. *Nat. Commun.* **2013**, *4*, 2551.

(33) Chilton, N. F.; Langley, S. K.; Moubaraki, B.; Soncini, A.; Batten, S. R.; Murray, K. S. *Chem. Sci.* **2013**, *4*, 1719−1730.

(34) Yamamoto, K.; Funasaka, H.; Takahashi, T.; Akasaka, T.; Suzuki, T.; Maruyama, Y. *J. Phys. Chem.* **1994**, *98*, 12831−12833.

(35) Wakahara, T.; Kobayashi, J.; Yamada, M.; Maeda, Y.; Tsuchiya, T.; Okamura, M.; Akasaka, T.; Waelchli, M.; Kobayashi, K.; Nagase, S.;

DOI: 10.1021/jacs.6b04037
J. Am. Chem. Soc. 2016, 138, 8000−8006

Kato, T.; Kako, M.; Yamamoto, K.; Kadish, K. M. *J. Am. Chem. Soc.* **2004**, *126*, 4883−4887.
(36) Francl, M. M.; Pietro, W. J.; Hehre, W. J.; Binkley, J. S.; Gordon, M. S.; Defrees, D. J.; Pople, J. A. *J. Chem. Phys.* **1982**, *77*, 3654−3665.
(37) Binkley, J. S.; Pople, J. A.; Hehre, W. J. *J. Am. Chem. Soc.* **1980**, *102*, 939−947.
(38) Petersson, G. A.; Bennett, A.; Tensfeldt, T. G.; Allaham, M. A.; Shirley, W. A.; Mantzaris, J. *J. Chem. Phys.* **1988**, *89*, 2193−2218.
(39) Cao, X. Y.; Dolg, M. *J. Mol. Struct.: THEOCHEM* **2002**, *581*, 139−147.
(40) Barone, V. In *Recent Advances in Density Functional Methods, Part I*; Chong, D. P., Ed.; World Scientific Publ. Co.: Singapore, 1996.

DOI: 10.1021/jacs.6b04037
J. Am. Chem. Soc. 2016, 138, 8000−8006